Polymer 284 (2023) 126302

Contents lists available at ScienceDirect

Polymer

journal homepage: www.elsevier.com/locate/polymer

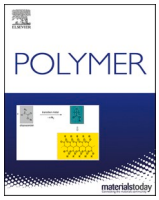

Thermally-triggered multi-shape-memory behavior of binary blends of cross-linked EPDM with various thermoplastic polyethylenes and their potential applications as temperature indicators

Reinhold Pommer [a,b], Robert Saf [a], Ralf Supplit [c], Armin Holzner [c], Harald Plank [d,e], Gregor Trimmel [a,*]

[a] Institute for Chemistry and Technology of Materials, Graz University of Technology, Stremayrgasse 9, 8010, Graz, Austria
[b] Polymer Competence Center Leoben GmbH, Roseggerstrasse 12, 8700, Leoben, Austria
[c] Semperit Technische Produkte Gesellschaft m.b.H, Triester Bunderstrasse 26, 2632, Wimpassing, Austria
[d] Institute of Electron Microscopy and Nanoanalysis, Graz University of Technology, Steyrergasse 17, 8010, Graz, Austria
[e] Austrian Centre for Electron Microscopy, Steyrergasse 17, 8010, Graz, Austria

ARTICLE INFO

Keywords:
Shape-memory polymers (SMPs)
Stimuli-responsive materials
Multi-shape-memory
Elastomer-thermoplastic-blends
Temperature indication
Thermomechanical properties

ABSTRACT

Shape-memory polymers (SMPs) are smart materials that can alter their configuration in response to external stimuli. They have shown promise in a number of application areas, including soft robotics or biomedical devices. Frequently, however, the materials needed are expensive, or labor-intensive synthetic processes are involved. In this contribution, we report a versatile and cost-effective manufacturing method for SMPs based on binary elastomer-thermoplastic-blends. These were produced from ethylene-propylene-diene monomer rubber (EPDM) combined with ultra-low-density polyethylene (ULDPE), propylene-ethylene copolymer (PP-c-PE), or high-density polyethylene (HDPE) as thermoplastic components. Atomic force microscopy revealed an immiscible two-phase morphology. Results of dynamic-mechanical thermal analysis showed that all polymer blends with a high thermoplastic load had efficient thermo-responsive dual-shape-memory, also demonstrated on macroscopic specimens. Furthermore, multi-shape-memory of elastomer/thermoplastic (40/60)-blends was investigated. Especially ULDPE-containing blends exhibited particularly promising multi-shape-memory features and stepless, controllable temperature response. Mechanistically, this is based upon the synergistic interaction of the cross-linked elastomer and the thermoplastic switching phase, consisting of different crystalline segments melting over a wide range from 60 to 125 °C. The continuous shape recovery over a broad temperature range could be used to create reusable test strips, e.g., for indicating exposure temperature in transportation chains or overheating protection.

1. Introduction

Shape-memory polymers (SMPs) are a category of smart materials with the ability to recover from one or multiple temporary shape deformations into a permanent configuration upon exposure to external stimuli [1–3]. This phenomenon is referred to as shape-memory effect (SME). Electricity, magnetism, irradiation, solvents, chemical reactions, and especially temperature are examples of triggers that are either specifically targeted or result from environmental changes, opening up potential applications in various fields [4–15]. Thermo-responsive materials have received the most attention among SMPs. Highly efficient dual-shape-memory behavior can be realized through the synthesis of novel segmented polymers, composites, supramolecular networks, or polymer blends [5,16–20]. More recently, multi-shape-memory polymers (MSMPs) that can fix two or more temporary shapes have piqued the interest of researchers [21–25].

The underlying shape fixation and recovery mechanism relies on the interaction of a fixed phase with reversible switching domains. The permanent shape is determined by chemical or physical cross-links in the fixed phase, whereas the thermal transitions of the switching domains (melting or glass transition) ensure dual- or multi-shape-memory behavior by locking the temporary shapes [26–28]. This is usually achieved by applying a defined mechanical deformation above the transition temperature (T_{trans}) and subsequent quenching below T_{trans}

* Corresponding author.
E-mail address: gregor.trimmel@tugraz.at (G. Trimmel).

https://doi.org/10.1016/j.polymer.2023.126302
Received 26 May 2023; Received in revised form 23 August 2023; Accepted 24 August 2023
Available online 24 August 2023

under the applied load. The solidification of the switching domains along the oriented network of the permanent phase allows for the fixation of the deformed shape during this process [17,27–29]. The energy input from the applied load is simultaneously stored by the elastic component's reconfiguration. The fixing integrity of the switching domains is lost when this process is reversed by reheating above T_{trans}. Thus, the original shape is recovered using the retractive force [17,27,30]. It should be noted that even if the initial shape is quantitatively recovered, all other macroscopic physical and thermal properties might not be fully restored. This is attributed to the occurrence of irreversible microstructural changes in the material and is frequently subordinated to the shape-memory efficiency or ignored depending on the operation purpose.

For a long time, the majority of investigated SMPs were prepared through chemical synthesis and modifications to create integrated systems that combine fixing and switching segments in a single polymer or network. These include, e.g., chemically linked polymer networks, side chain design, but also the preparation of segmented block-copolymers [31–33]. While these routes are often resource- and labor-intensive, the blending of readily available materials can be a cost-efficient and convenient alternative for the fabrication of dual- and multi-SMPs exhibiting thermo-responsive shape-memory behavior. Consequently, interest in various types of miscible and immiscible polymer blends has increased recently [17,34,35]. Gao et al. [36] described efficient multi-shape-memory blends of various polyolefin elastomers (POE) that exploit physical cross-links to recover their permanent shape. Similarly, Tekay et al. [37] achieved efficient SME by manufacturing poly (ethylene-co-1-octene) and poly (styrene-b-isoprene-b-styrene) thermoplastic-elastomer-blends. Zhang et al. [38] recently reported the preparation of triple-shape-memory ternary blends using POEs, poly (caprolactone) (PCL), and lauric acid (LA), whereas others used secondary interactions to create tunable shape-memory in ternary mixtures consisting of thermoplastic polyurethane (TPU), polylactic acid (PLA), and poly (propylene carbonate) (PPC) [39]. There have been fewer recent studies dealing with SMPs based on chemically cross-linked blends and networks. In some instances, rubber-thermoplastic-blends were prepared as TPVs (thermoplastic vulcanizates): Chen et al. reported thermally triggered SMPs based on binary blends of PLA and ENR (epoxidized natural rubber), exhibiting a sea-island structure, produced via peroxide cross-linking [40]. Similarly, dynamically vulcanized and compatibilized EPDM-PP-blends with shape-memory behavior were studied by Xu et al. [41] Further rubber-thermoplastic-SMP-blends, i.e., based on EPDM or natural rubber in combination with different thermoplastics, were reported by the groups of Chatterjee and comprehensively reviewed by others [42,43]. As an example, EPDM and ethylene-octene-copolymer (EOC)-blends were used by Chatterjee et al. for dual-shape-memory materials. Dual- and triple-shape-memory was also demonstrated for cross-linked polyethylene blends and polyisoprene-paraffin mixtures [44,45]. Quadruple-shape-memory of 3D-printable ternary-blends was demonstrated by Chen et al. [46] Reports of MSMP based on elastomer-thermoplastic-blends that exhibit more than triple- or quadruple-shape-memory are rare.

It should be mentioned, that cross-linked semi-crystalline EPDM exhibits a certain shape-memory effect, as discussed in two recent studies by Wang et al. [47,48] Recently, Min et al. and Li and coworkers also demonstrated that the pure thermoplastics, i.e., semi-crystalline ultra-high molecular weight PE (UHMWPE) showed continuous shape-memory behavior in a temperature window between 90 °C and 138 °C, which was assigned to a rather broad range of the melting transition [49,50].

The aim of this contribution is to describe a versatile method for the production of SMPs based on elastomer-thermoplastic-blends by combining EPDM with either ultra-low-density polyethylene (ULDPE), which is an ethylene-1-hexene copolymer, propylene-ethylene copolymer (PP-c-PE), or high-density polyethylene (HDPE), respectively. The developed materials exhibit interesting mechanical properties as well as excellent thermally-triggered dual- and triple-shape-memory features. The broad thermal transition of ULDPE allows the realization of even a multi-shape material with respectable shape-fixity and recovery values for phase-separated EPDM/ULDPE (40/60)-blends. The temperature-triggered shape recovery that proceeds well-controlled across a broad transition range could be applied to create reusable test strips for exposure temperature indication e.g., applicable for transportation chains or overheating protection.

2. Experimental section

2.1. Materials

Semi-crystalline EPDM Nordel™ IP 4760 (ethylene content of 65.5–69.5 wt%, ENB (ethylidene norbornene) content of 4.5–5.3 wt%), propylene-ethylene copolymer (PP-c-PE, VERSIFY™ 2300) and ultra-low-density poly (ethylene-hexene) copolymer (ULDPE Attane™ 4607 GC) were all from Dow Chemical Company (USA). High-density polyethylene (HDPE Borsafe HE3490) was purchased from Borealis (Austria). Zink oxide (ZnO) and stearic acid (SA) were used as vulcanization activators; ground sulfur (S_8), accelerators *N*-cyclohexyl-2-benzothiazole sulfenamide (CBS), tetramethylthiuram disulfide (TMTD) and diphenyl guanidine (DPG) were used as cross-linking agents. Chemicals were provided in technical grades by Semperit Technische Produkte GmbH (Austria). All materials were processed without further modification or purification.

2.2. Sample preparation

EPDM/thermoplastic-blends were prepared by a three-step process, including the blending of the raw materials, the addition of curatives, and hot-press vulcanization. Initial mastication and melt-blending of the corresponding raw materials in different ratios was realized using a Plasti-Corder internal mixer (Brabender, Germany). Elastomer/thermoplastic-blends with mixing ratios of 70/30, 50/50 and 40/60 (wt/wt) were investigated, where the thermoplastic is either ULDPE, PP-c-PE or HDPE. Mixing was carried out at a temperature of 140 °C for 5 min at a rotor speed of 75 rpm. Activating compounds (6.2 phr ZnO and 1.3 phr stearic acid) were directly added to the mixture in the compounder, resulting in batch sizes of approximately 60 g. Cross-linkers and accelerators for sulfur-based vulcanization were mixed into the batches on a two-roll mill (Servitec, Germany) at room temperature: 0.7 phr ground sulfur and the accelerator system (CBS, TMTD, DPG) with a total of 4 phr. Quantities given in phr (parts per hundred parts rubber) are with respect to the amount of EPDM used in the respective batch. The samples investigated in this work, as well as the corresponding formulations, are listed in Table 1. Denotation E/T describes the EPDM/thermoplastic ratio in wt/wt. After storage overnight, the vulcanization characteristics were determined using a Rheoline Multifunction moving-die rheometer (Prescott Instruments, UK). All tests were carried out at 190 °C (constant frequency = 1.67 Hz,

Table 1
Formulations of EPDM/thermoplastic-blends, where E/T indicates the ratio EPDM/thermoplastic. Quantities are given in parts per hundred parts rubber (phr) with respect to the amount of EPDM in the batch.

Component	Sample			
	E (100)	E/T (70/30)	E/T (50/50)	E/T (40/60)
EPDM [phr]	100	100	100	100
Thermoplastic[a] [phr]		43	100	150
ZnO [phr]	6.2	6.2	6.2	6.2
Stearic acid [phr]	1.3	1.3	1.3	1.3
Sulfur [phr]	0.7	0.7	0.7	0.7
Accelerator system [phr]	4.0	4.0	4.0	4.0

[a] Thermoplastic = ULDPE, PP-c-PE or HDPE.

oscillation angle = 0.50°). Data of rheological measurements are shown in the supplementary information (Fig. S1). Subsequently, vulcanization was performed by hot-press molding at 190 °C for 10 min, utilizing a Collin P 200 PV electrical press (Collin, Germany). Sample sheets with a thickness of ca. 1.5–2 mm were prepared.

2.3. Characterization

2.3.1. Mechanical testing

An Autograph AGS-X 5 universal tensile tester (Shimadzu, Japan) was used to determine the physico-mechanical properties, primarily tensile strength and ultimate elongation, of the blends at room temperature. Uniaxial tensile tests were performed at a strain rate of 500 mm min^{-1} (no pre-load) on shouldered test bars (total length = 100 mm, clamping length = 75 mm, width = 3 mm). Specimen thickness was determined using a Digimatic Micrometer (Mitutoyo, Japan).

2.3.2. Differential scanning calorimetry

Differential scanning calorimetry (DSC) measurements were performed in the thermal range of −60 to 160 °C on a DSC 214 Polyma (Netzsch, Germany) and a double furnace DSC 8500 (PerkinElmer, USA). Melting transitions were determined from heating cycles at a rate of 10 K min^{-1} and crystallinity values were calculated from cooling cycles at a rate of 10 K min^{-1} under nitrogen atmosphere. Melting and glass transition temperatures were defined by peak point and inflection point values from heat flow curves, respectively.

2.3.3. Atomic force microscopy

Atomic force microscopy (AFM) was conducted to study morphology, micro-structural phase separation and qualitative mechanical aspects. Samples for AFM (EPDM/ULDPE-blends) were prepared without activating agents (ZnO, stearic acid), otherwise analogously. Cross-linked EPDM/ULDPE in distinct ratio variations of 75/25, 40/60 and 25/75 (wt/wt) were examined. Cross-sectional samples were prepared by ultramicrotomy at cryogenic temperatures of −150 °C with cooling/heating times from/to room temperature of at least 90 min. All samples were immediately subjected to AFM measurement in tapping mode, using a FastScanBio platform (Bruker Nano, USA) with nominal cantilever spring constants around 26 N m^{-1} in soft repulsive conditions. To ensure reliability, at least three different regions were characterized and analyzed. Post-processing was minimized to 1st order flattening, followed by statistical analyses using the NanoScope Analysis software package (V1.8, Bruker Nano, USA).

2.3.4. Dynamic-mechanical thermal analysis

Thermomechanical behavior and shape-memory properties were investigated via DMTA (dynamic-mechanical thermal analysis) on a DMA Q800 (TA Instruments, USA) equipped with tension clamps. Specimens had rectangular geometry (length/width/thickness approx. 25 mm/5.3 mm/1.5 mm, clamping length approx. 10 mm). Programming of the DMTA was adjusted to the corresponding materials and characteristics of interest; control parameters were chosen accordingly. The specific procedures are described below.

2.3.4.1. Procedure for dual-shape-memory cycles. The following sequence was used to investigate the thermally-triggered dual-shape-memory behavior of the EPDM/thermoplastic-blends: 1) Application of a minimal force F_{min} of 1 mN, which was generally used in all "unloaded" steps of the sequence. This force turned out to be too small to influence the strain behavior of the investigated blends significantly, but improved data quality (e.g., reduced noise). 2) Thermal equilibration at T_{low} = 20 °C. 3) Heating of the specimen to the transition temperature T_{trans} = 140 °C. 4) Increase of the strain to ε_{load} = 50%. 5) Cooling of the sample under load to T_{low} = 20 °C for shape-fixation. 6) Unloading of the sample (F_{min} = 1 mN) for determination of the fixed strain (ε_{fix}). 7) Shape recovery by reheating the specimen to T_{trans} for determination of recovered strain (ε_{rec}). Heating/cooling rates were generally 10 °C min^{-1}. Additionally, for thermal and creep/recovery equilibration, isothermal delays of 15 min were implemented after steps 2, 3, 6, and 7, respectively, and 30 min after steps 4 and 5. Steps 4 to 7 were repeated three times.

Shape-fixity ratios (R_f) and shape-recovery ratios (R_r) were calculated with data from the third shape-memory cycle (N = 3) according to Equations (1) and (2), respectively, where $\varepsilon_{load}(N)$, $\varepsilon_{fix}(N)$, and $\varepsilon_{rec}(N)$ are the strains of the sample in cycle N. $\varepsilon_{rec}(N\text{-}1)$ is the strain at the end of the preceding cycle (=the initial strain of cycle N).

$$R_f(N) = \frac{\varepsilon_{fix}(N)}{\varepsilon_{load}(N)} * 100\% \quad (1)$$

$$R_r(N) = \frac{\varepsilon_{load}(N) - \varepsilon_{rec}(N)}{\varepsilon_{load}(N) - \varepsilon_{rec}(N-1)} * 100\% \quad (2)$$

2.3.4.2. Procedure for slow thermo-responsive shape recovery with incremental temperature increase. The following sequence was used for the investigation of all 40/60-blends: 1) Application of a minimal force F_{min} of 1 mN. 2) Thermal equilibration at T_{low} = 20 °C. 3) Heating to T_{trans} = 140 °C at a rate of 10 °C min^{-1}, followed by 15 min isothermal. 4) Increase of the strain to ε_{load} = 50%. 5) Cooling (rate 10 °C min^{-1}) of the sample under load to T_{low} = 20 °C for shape fixation. 6) Unloading of the sample (F_{min} = 1 mN) for determination of the fixed strain (ε_{fix}). 7) Shape recovery by stepwise increase in the temperature to 140 °C in increments of 2.5 °C, with 20 min isothermal for equilibration after each increment. Additionally, isothermal delays of 30 min were implemented after steps 4), 5), and 6), respectively.

2.3.4.3. Procedures for the investigation of multi-shape-memory behavior

2.3.4.3.1. Detailed investigation of EPDM/ULDPE (40/60). The procedure consisted of the following steps (heating/cooling rates were generally 10 °C min^{-1}, isothermal steps are abbreviated with *x-iso*, with x being the time in min): 1) Application of a minimal force F_{min} of 1 mN. That force was again used for all "unloaded" steps. 2) Thermal equilibration at T_{low} = 20 °C. 3) Heating to T_{trans} = 140 °C. 4) 5 times the sequence: *15-iso*, application of $stress_n$, *30-iso*, cooling to T_n, *30-iso*, unloading of the sample. Within this loop, the following five pairs of $stress_n/T_n$ (N mm^{-2}/°C) were applied: n = 1: 0.04/120, n = 2: 0.085/100, n = 3: 0.175/80, n = 4: 0.35/60, n = 5: 0.70/20.5) *15-iso*. 6) Stepwise heating of the sample to 60, 80, 100, 120, and 140 °C, respectively. Each increase in temperature was followed by *30-iso*. A second shape-memory cycle was started, going back to loading of the sample with 0.04 N mm^{-2} at 140 °C. Deformation, fixation and recovery temperatures were selected between 60 and 120 °C in order to cover the full range of the material's broad thermal transition.

2.3.4.3.2. Comparative study of the 40/60-blends of EPDM with PP-c-PE, ULDPE, and HDPE. The sequence described above was used without intermediate unloading of the sample during stepwise cooling/shape programming. In the case of EPDM/PP-c-PE (40/60) the following values were applied for $stress_n$ (N mm^{-2}): n = 1: 0.04, n = 2: 0.06, n = 3: 0.08, n = 4: 0.10, n = 5: 0.12. For EPDM/HDPE (40/60), $stress_n$ (N mm^{-2}): n = 1: 0.04, n = 2: 0.375, n = 3: 0.75, n = 4: 1.125, n = 5: 1.50. All temperatures remained unchanged.

2.3.5. Shape-memory experiments on macroscopic samples

For demonstration purposes, the shape-memory or shape-morphing behavior was investigated qualitatively with a series of macroscopic samples with different geometries, preferably rectangular strips with a thickness of up to 2 mm. Samples were programmed into different, arbitrary geometries above the corresponding transition temperature(s) (T_{trans}). For dual-shape experiments, the deformation was performed at T_{trans} = 140 °C, and for triple-shape-memory at $T_{trans,1}$ = 140 °C and $T_{trans,2}$ = 60 °C. Temperatures were chosen according to the thermal

properties: at 140 °C (first deformation step), the thermoplastic component was typically fully melted, and at 60 °C, the crystalline segments of the EPDM were melted (allowing for the second shape fixation). The process is shown schematically in Fig. 4E. Programming and recovery steps were carried out in a heating cabinet or heated silicone oil bath, respectively.

2.3.6. Application of elastomer-thermoplastic-blends as temperature probing materials

The apparently stepless thermal shape-morphing features of the investigated blends, especially EPDM/ULDPE (40/60), open the possibility for application as temperature-probing materials, which can indicate a maximum exposure temperature by strain recovery to a defined and reproducible length. Sample strips of EPDM/ULDPE (length/width/thickness ca. 100 mm/10 mm/1.5 mm) were cut from vulcanized sheets and a defined length $L_0 = 80$ mm was marked on the samples. First, the samples were subjected to an initial shape-memory-cycle (140 °C, 50% strain) to erase the thermal history, and subsequently, the initial shape for the temperature-probing experiments was prepared by heating the strips to 140 °C and fixing a temporary deformation of 120 mm (50% strain). These were then exposed to different temperatures between 60 °C and 140 °C, either by incremental temperature increase (10 °C-steps) or by directly heating to certain target temperatures, while measuring the recovered strain after the treatment.

3. Results and discussion

3.1. Blend preparation and mechanical properties

The beneficial effect of blending elastomers with thermoplastic materials, i.e., polyolefins, on general mechanical performance, as well as their blend morphology, has been thoroughly investigated and established [51–58]. Fig. 1A depicts the three-step manufacturing route, used to prepare the binary EPDM-thermoplastic-blends. Initial melt-mixing resulted in macroscopically homogenous, miscible batches, to which curatives were later added on a two-roll mill at room temperature. Finally, the cross-linking of the EPDM phase was initiated during the static vulcanization process, using an electrical hot-press. At the molecular level, sulfide cross-links between the EPDM chains, more precisely between the unsaturated bonds of the norbornene units, are generated. Thus, an elastomeric phase was formed, embedding the thermoplastic component, resulting in a binary, yet macroscopically compatible and stable blend. The interconnected fixed elastomer network is crucial for the elastic behavior and effectively driving the shape recovery process. The influence of the blending ratio of the produced EPDM/ULDPE-, EPDM/PP-c-PE- and EPDM/HDPE-systems on the mechanical properties while maintaining a consistent cross-linking formulation was investigated by standardized uniaxial tensile testing. Figs. 1C to D show representative stress-strain-curves for EPDM/PP-c-PE-, EPDM/ULDPE- and EPDM/HDPE-blends, respectively, depicting also the pure corresponding thermoplastic component and the cross-linked pure rubber.

PP-c-PE, which, from its structural nature, has more elastic features than all other applied polyolefins, showed a lower initial modulus at low strain, followed by strain hardening up to the rupture point. EPDM/PP-c-PE-blends expectedly revealed a more rubber-like stress-strain curve, with blends with a higher thermoplastic loading having similar characteristics to the pure PP-c-PE, with only small variations in ultimate values. Pure ULDPE exhibited a plastic deformation curve with a narrow linear elastic region, a somewhat pronounced yield point and apparent strain hardening at higher elongations. EPDM/ULDPE-blends in a ratio of 40/60 and 50/50 showed ultimate properties (elongation and tensile strength), which were very comparable to pure ULDPE. The elastic behavior of the blends in comparison with pure ULDPE was much more pronounced, which was attributed to the elastomeric compound. With a higher elastomer content (70/30-blends), the blend properties approached the values of the pure EPDM-component with a significantly decreased elongation at break and ultimate strength. For the shown EPDM/ULDPE- and EPDM/PP-c-PE-blends with a 50/50- and 40/60-ratio strain hardening, and even slightly pronounced hyperelastic

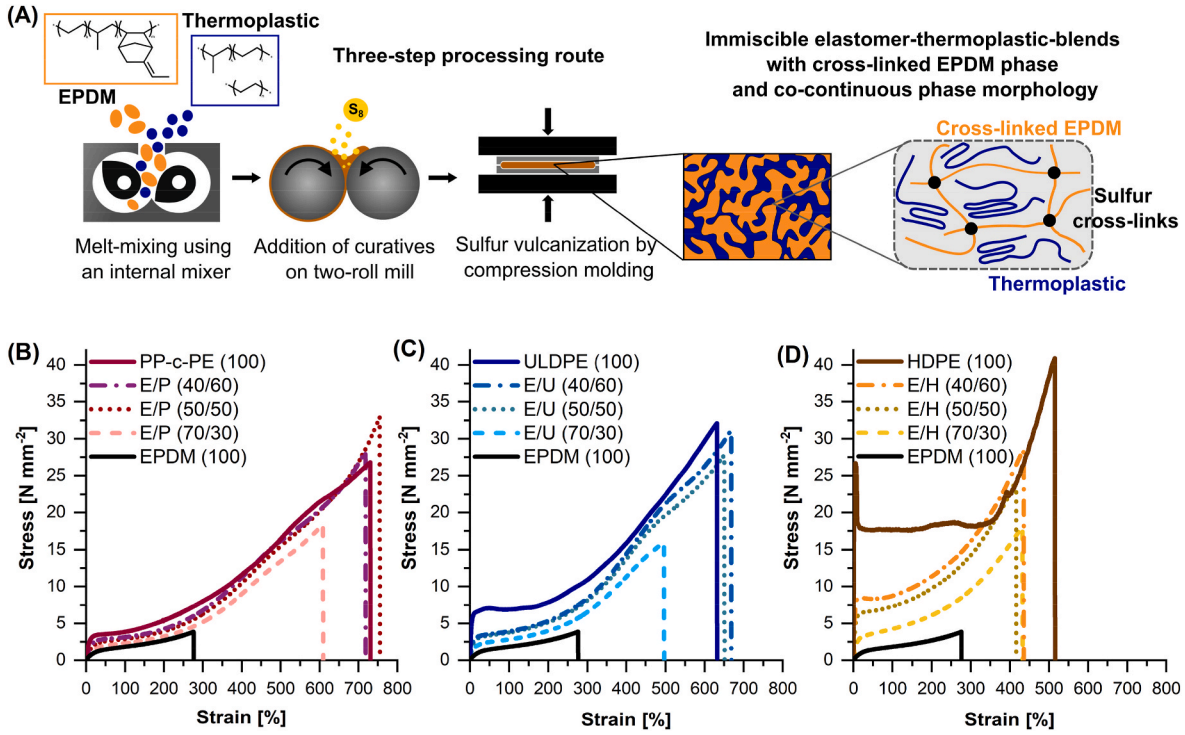

Fig. 1. Three-step processing route for the preparation of immiscible binary elastomer-thermoplastic-blends with a sulfur-cross-linked EPDM phase **(A)**. Comparison of stress-strain curves for EPDM/PP-c-PE- **(B)**, EPDM/ULDPE- **(C)** and EPDM/HDPE-blends **(D)** as function of the elastomer/thermoplastic blending ratio, as well as the corresponding elastomer and thermoplastic materials.

behavior could be observed. Pure HDPE displayed a typical thermoplastic stress-strain curve, with an initial yield stress of 26 N mm^{-2} (at 5% strain) and an extended plastic region of approximately 400%. EPDM/HDPE-blends showed significantly different curves, in which the ductile characteristics had practically disappeared. EPDM/HDPE (40/60) exhibited a barely noticeable yield point; higher EPDM-loading led to samples with a more elastic behavior and strain-hardening effects, which generally had lower ultimate elongations compared to their ULDPE and PP-c-PE counterparts. Owed to the interconnected, cross-linked EPDM phase, all blends displayed elastic or elastomeric behavior to some extent. With a shift in the blending ratio towards a higher thermoplastic content, elastomeric behavior consequently steadily diminished.

Table 2 summarizes all corresponding mechanical key characteristics resulting from the performed tensile tests, including tensile strength, elongation at break and Young's Moduli. The cross-linked pure EPDM sample reached a tensile strength of less than 4 N mm^{-2} and an ultimate elongation of 280%. These moderately low values for the pure, semi-crystalline rubber can be attributed to a rather densely cross-linked network. Generally, a network with a predominance of short cross-links (especially mono- and di-sulfide bonds) and a comparably low portion of polysulfide links has to be expected with the applied curative formulation combined with prolonged vulcanization times [59,60].

Adding only 30 wt% of thermoplastic component already significantly improved the tensile strength to 19.6 N mm^{-2} when using PP-c-PE and 16.4 N mm^{-2} with ULDPE. Likewise, the elongation at break increased to 625% and 501% for PP-c-PE- and ULDPE-blends, respectively. EPDM/PP-c-PE (70/30 and 50/50)- blends exhibited superior tensile strength and elongation at break, effectively yielding almost 33 N mm^{-2} and 750% at a ratio of 50/50 (wt/wt). Up to this blending ratio, the PP-c-PE-blends apparently outperformed their ULDPE counterparts. However, subsequently, the performance slightly dropped when the PP-c-PE content was raised to 60 wt%. This might be attributed to a change in overall blend morphology and impaired load transfer. The 40/60-specimen showed mechanical properties close to those of pure PP-c-PE, which supports this assumption. In contrast to PP-c-PE-samples, the EPDM/ULDPE-blends yielded continuously improved values up to a ratio of 40/60 (wt/wt) reaching a maximum tensile strength of 31 N mm^{-2} and an elongation of 670% with the highest investigated ULDPE loading. The tensile strength of the 40/60-blend was quite similar when compared to pure ULDPE.

This general enhancement of mechanical characteristics demonstrated the reinforcing nature of the thermoplastic in the mixture. It further proves the strong dependency on the blending ratio, which ultimately dictates the blend morphology and the load transfer between the phases [51,57,61]. An approach for a general understanding of the origin of polyethylene's reinforcing effects in ULDPE/EPDM blends has been described previously [62]. The mechanical properties of both, EPDM-blends with PP and PE, have been the subject of various studies [63–67]. Strong strain hardening of pure HDPE above 380% resulted in rupture at 40 N mm^{-2} with an ultimate elongation of 511%. EPDM/HDPE-blends in different ratios showed very similar ultimate elongations, with values slightly above 400%. Tensile strength increased with the thermoplastic loading from EPDM/HDPE (70/30), from 17 N mm^{-2} up to 28 N mm^{-2} for the 40/60-blends. A comparison of Young's Moduli facilitated a clear distinction between the three used thermoplastic compounds: EPDM/PP-c-PE-blends, which constituted the comparatively softest material combination, showed moduli between 12 and 23 N mm^{-2} (70/30- and 40/60-blend respectively). EPDM/ULDPE-blends reached up to 51 N mm^{-2}, while EPDM/HDPE--blends' highest moduli were found at 223 N mm^{-2}. Additionally, consequential results for moduli at different elongations (M50, M100, M300) are summarized in Table S1. It is also important to consider the elastic moduli of the blended materials because most of the performed shape-memory deformations fall within the range of 50–100% elastic deformation. Increased thermoplastic compounds in EPDM/thermoplastic-blends naturally result in a higher modulus in both blend systems, raising the elastic material's initial stiffness.

Table 2
Tensile strength, elongation at break and Young's Moduli for EPDM/PP-c-PE-, EPDM/ULDPE- and EPDM/HDPE-blends with different blending ratios.

EPDM/PP-c-PE [wt/wt]	Tensile strength [N mm^{-2}]	Elongation at break [%]	Young's Modulus (E) [N mm^{-2}]
100/0	3.85 ± 0.5	278 ± 24	6.2 ± 0.3
70/30	19.6 ± 1.7	625 ± 23	12 ± 1
50/50	32.8 ± 1.0	749 ± 15	19 ± 1
40/60	28.4 ± 1.9	717 ± 24	23 ± 1
0/100	27.7 ± 1.9	741 ± 25	36 ± 1
EPDM/ULDPE [wt/wt]	Tensile strength [N mm^{-2}]	Elongation at break [%]	Young's (E) Modulus [N mm^{-2}]
70/30	16.4 ± 2.8	501 ± 57	21 ± 1
50/50	27.6 ± 1.9	644 ± 24	38 ± 3
40/60	31.3 ± 2.5	671 ± 31	51 ± 4
0/100	32.2 ± 1.3	635 ± 17	124 ± 5
EPDM/HDPE [wt/wt]	Tensile strength [N mm^{-2}]	Elongation at break [%]	Young's Modulus (E) [N mm^{-2}]
70/30	17.0 ± 2.7	411 ± 41	40 ± 1
50/50	24.4 ± 1.8	408 ± 15	138 ± 5
40/60	27.6 ± 2.2	428 ± 18	223 ± 13
0/100	40.0 ± 1.9	511 ± 4	921 ± 18

3.2. Thermal properties and thermodynamic compatibility

Overall mechanical properties of polymer blends are evidently dependent on the chemical and structural properties of the raw components, the blending ratio, their morphology and their thermodynamic compatibility. These factors determine whether the components form a fully miscible, partially miscible, or immiscible (i.e., phase separated) system [55,68–71]. Differential scanning calorimetry (DSC) was used to determine the thermal transition temperatures of the materials and to evaluate the thermodynamic compatibility in terms of miscibility of the semi-crystalline polymer blends. Representative DSC curves (heating rate 10 K min^{-1}) for the pure thermoplastic compounds, processed EPDM and 40/60-blends of EPDM/thermoplastic are shown in Fig. 2. As mentioned in the experimental section, the EPDM type used contained a relatively high ethylene content (65.5–69.5 wt%) and is therefore semi-crystalline. Accordingly, this compound showed two temperature transitions in the measurement range: the first transition was observed at −49 °C, which corresponds to the glass transition (T_g). The second was the melting transition (T_m) between 29 and 48 °C (peak maximum at 38 °C). Fig. 2A shows the heating curves for PP-c-PE and the corresponding EPDM/PP-c-PE-blend; Fig. 2B includes pure ULDPE and EPDM/ULDPE, and HDPE and EPDM/HDPE are presented in Fig. 2C. The pure propylene-ethylene copolymer (PP-c-PP) revealed a T_g at −28 °C and two separate melting ranges: 30–75 and 115–145 °C, with peak maxima at 47 °C and 135 °C, respectively. In contrast to that, the pure ULDPE copolymer exhibited an initial temperature transition between 30 and 45 °C, a broad melting transition range with an onset at about 45 °C and three distinct melting peak maxima at 56, 101 and 121 °C. A clear T_g was not observed.

Regarding the EPDM/PP-c-PE-blend, a $T_{g,1}$ at −50 °C could be assigned to the rubber phase and a $T_{g,2}$ at −32 °C originated from the thermoplastic component. A broad melting peak starting at ca. 28 °C was observed, attributed to a superposition of melting transitions from both phases. A second melting transition, corresponding to PP-c-PE, was found to be at 135–145 °C ($T_{m,peak}$ = 142 °C). EPDM/ULDPE (40/60) revealed a T_g of −50 °C, stemming from the rubber phase. The transition of the blend with a maximum at 45 °C was primarily attributed to the crystalline segments of EPDM, but also to the first melt transition of ULDPE. The melting process of ULDPE then continues up to a temperature of 123 °C. For raw HDPE a sharp melting transition in the range of

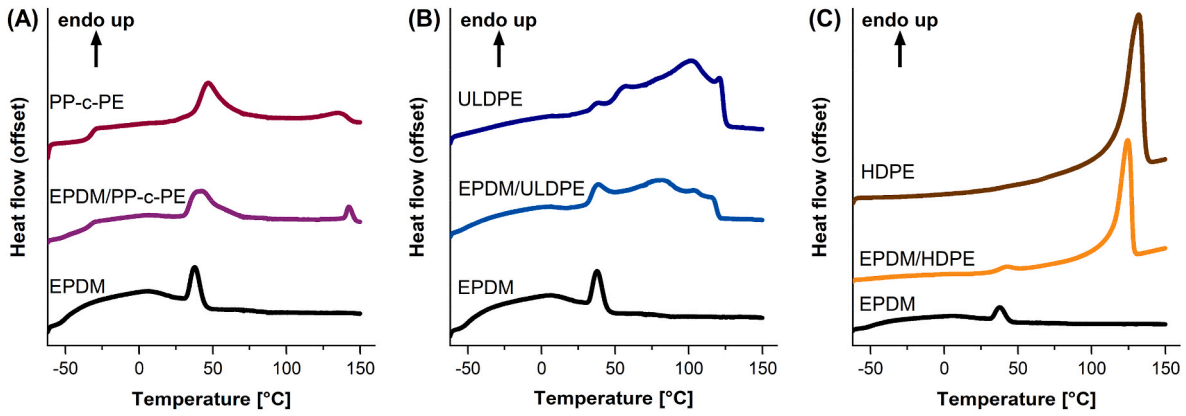

Fig. 2. DSC heating curves (endothermic up) of cross-linked EPDM/PP-c-PE- **(A)**, EPDM/ULDPE- **(B)** and EPDM/HDPE-blends **(C)**, each in a 40/60-ratio, and the corresponding pure materials. Scaling of the heat flow axis in **(C)** differs because of the greater heat flow resulting from the high crystallinity of HDPE.

115–138 °C ($T_{m,peak}$ = 131 °C) was observed. The appearance of this distinct peak remained vastly unchanged in the EPDM/HDPE (40/60)-blend ($T_{m,peak}$ = 125 °C). At 30–50 °C the transition corresponding to the EPDM phase was found. Gathered thermal data is additionally summarized in the supporting information (Table S2). Comparing the thermal transition temperatures (T_g and T_m-values) of the respective single components and the blends produced therefrom, no significant shifts were observed. This strongly suggests that the elastomer-thermoplastic-blends were phase-separated, which was obviously favorable regarding the presumed underlying mechanism for shape-memory behavior [72,73]. Supplementary DSC data, including measurements on blends in all different ratios (70/30, 50/50 and 40/60) in comparison to their corresponding raw constituents, are made available (see supporting information, Fig. S3). No significant shifts in the position of glass- and melting transitions could be observed, signifying that these were largely unaffected by the blending ratios. Hence, the useable transition temperature for the SMP-blends in different ratios remained unchanged, as all mixtures constituted immiscible systems.

3.3. Phase morphology of EPDM/ULDPE-blends

To evaluate miscibility, phase separation and internal morphology of EPDM/ULDPE-blends, tapping mode AFM measurements were conducted with a focus on qualitative mechanical mapping via phase imaging. Experience had shown that certain components, such as metal oxide particles or fillers, hindered an immaculate sample preparation as well as negatively influenced the measurement. Therefore, samples for AFM were especially and freshly prepared without the application of activating agents (ZnO and stearic acid), to optimize sample preparation by ultramicrotomy and to avoid interfering particles and additional artifacts. More distinct blend ratios of 75/25, 40/60 and 25/75 (wt/wt) were used, to enhance the contrast and allow for a clear phase identification of the elastomer and thermoplastic phases.

Fig. 3 gives a direct comparison for 75/25 **(A)**, 40/60 **(B)** and 25/75 **(C)** blend ratios with decreasing scan widths of 10 µm, 5 µm and 1 µm (from left to right). As evident, the cross-linked blends revealed clear phase separations, which was in agreement with literature [61,68,70,71,

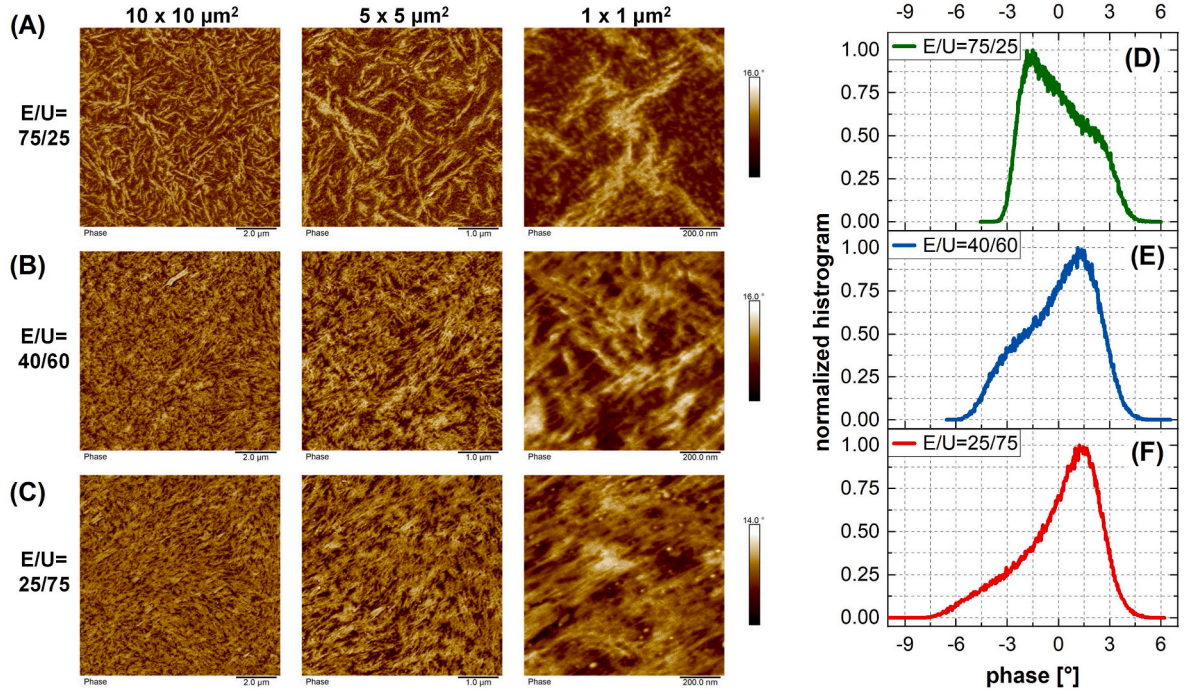

Fig. 3. 10 × 10 µm², 5 × 5 µm² and 1 × 1 µm² AFM phase images of cross-linked EPDM/ULDPE blends with a ratio of 75/25 **(A)**, 40/60 **(B)** and 25/75 **(C)** with representative, normalized histograms **(D–F)**, taken from 5 × 5 µm² phase maps.

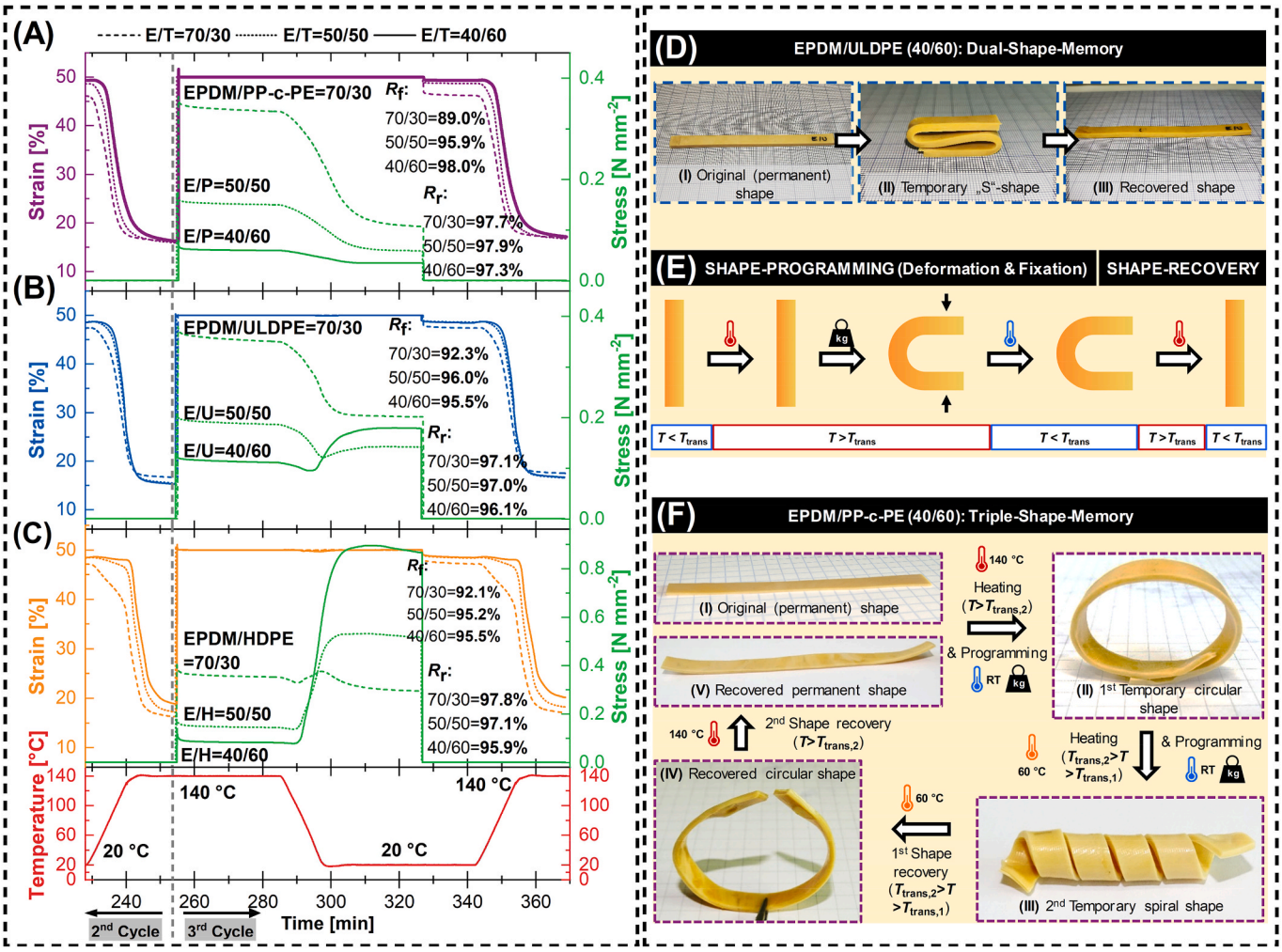

Fig. 4. DMTA data showing the dual-shape-memory experiment (3rd cycle) of EPDM/PP-c-PE-blends **(A)**, EPDM/ULDPE-blends **(B)** and EPDM/HDPE-blends **(C)**, respectively, with EPDM/thermoplastic (E/T)-ratios of 70/30 (dashed lines), 50/50 (dotted lines) and 40/60 (solid lines); shape deformation at T_{trans} = 140 °C and shape fixation at T_{min} = 20 °C. Graphs indicate shape-fixity ratios (R_f) and shape-recovery ratios (R_r) calculated according to Equations (1) and (2). Macroscopic (qualitative) example of dual-shape-memory on EPDM/ULDPE (40/60) with a temporary "S"-shape **(D)** and the schematic representation of the applied programming-recovery cycle **(E)**. Qualitative examples of triple-shape-memory on EPDM/PP-c-PE (40/60) with a temporary circular and spiral shape, respectively **(F)** with $T_{trans,1}$ = 140 °C and $T_{trans,2}$ = 60 °C, chosen according to the range of the thermoplastics' and EPDM's major melting transition, respectively.

74] and DSC data shown in the previous section. In the shown phase images, darker regions indicate softer material properties, which suggest them as EPDM phases. Brighter regions correspondingly represent the thermoplastic. To substantiate that claim, representative phase histograms are shown at the right, where the highest EPDM contents of 75 wt % (top row **A**) led to a histogram with two convoluted peaks **(D)**. Decreasing the EPDM content to 40 wt% **(B)** and 25 wt% **(C)**, the peak distributions in related histograms **E** and **F** changed as well, which supports the assumption, that darker parts correspond to the softer EPDM phase, while brighter parts indicate the thermoplastic ULDPE content. As becomes particularly evident in **A**, the ULDPE phase formed elongated morphologies, with a generally stochastic orientation. Higher contents revealed some preferred orientations (bottom left to top right) in 1 × 1 μm^2 phase scans, which, however, possibly stemmed from the ultramicrotome cutting direction. Having a look at 5 × 5 μm^2 and 10 × 10 μm^2 scans, the generally stochastic character of elongated ULDPE structures becomes again evident. Preceding studies of blends with EPDM-materials and PP-c-PE or HDPE in different blending-ratios have shown similar phase separated structures [75].

3.4. Fundamental shape-memory behavior

The thermo-responsive dual-shape-memory behavior was first investigated by DMTA, applying the method described in section 2.3.4.1. Based on the results obtained by DSC, T_{low} = 20 °C was selected as the lowest temperature for the fixation of shapes, and T_{trans} = 140 °C as transition temperature. This temperature was above the highest melting transition for all systems investigated within this work. Consequently, all thermoplastic phases should be in the molten state. Fig. 4A–C shows DMTA-data, obtained for the different blends of EPDM with PP-c-PE, ULDPE, and HDPE, respectively. For the corresponding 3D-representations, we refer to Figs. S5–S8. All graphs show data obtained during the third cycle. With respect to strain fixity, these data were substantially more comparable to those observed during the first and second cycles, while the stress necessary to reach ε_{load} = 50% was usually a bit higher in the first cycle, but again rather similar in the second (as an example, compare Figs. S4 and S5). The generally somewhat higher stress necessary during the first cycle was assigned to partial rearrangement of polymer segments as well as to the release of internal stress - originating from hot-press molding, vulcanization, subsequent cooling, sample cutting, etc., when the sample was stretched to a strain of 50% for the first time. Furthermore, at the end of the first cycle, after

thermally-triggered recovery, generally a significant remaining strain of several percent was observed. This was partially again assigned to the effects mentioned above, but also to some adaptation of the sample to the clamps when cycled for the first time. Accordingly, the first cycle was an annealing/conditioning step, and the graphs in Fig. 4A–C depicts the specific repeatable dual-shape-memory behavior of the blends.

In more detail, the graphs show that a strain of $\varepsilon_{load} = 50\%$ was applied 15 min after heating the blends from 20 to 140 °C ($t = 255$ min). After an equilibration/creep time of 30 min the stretched samples were cooled back to 20 °C to fix the temporary shape. Again, 30 min later, the stress was removed, which generally resulted in a small, abrupt drop of the strain, which was allowed to equilibrate for 15 min (ε_{fix}). Subsequently, smooth, gradual recovery of the samples occurred during the next heating step to 140 °C, and the strain remaining in the sample (ε_{rec}) was determined after 15 min equilibration.

Comparing the graphs, it becomes evident, that all blends could fix shape deformations quite well and thereafter also demonstrated efficient recovery. Blends containing more thermoplastic generally exhibited somewhat increased shape fixation; e.g., in the case of EPDM/PP-c-PE an improvement from 89.0% to 95.9% was observed when changing the EPDM/thermoplastic ratio from 70/30 to 50/50. The 40/60-blend remained at a strain fixity of 98.0%. This trend confirmed the suggested synergism of the distinct domains, where the thermoplastic phase promotes shape fixation. A bit surprising, even the relatively low amount of cross-linked EPDM in the 40/60-blend yielded respectable shape recovery, which appeared quite similar for all blend ratios (97.3–97.9%). Rather comparable behavior was seen for blends with ULDPE, where the shape-fixity ratio also increased significantly from 92.3% (70/30-blend) to 96.0% (50/50-blend). The somewhat smaller value of 95.5% observed for the 40/60-blend was assigned to accuracy limitations. Also, the rather tough EPDM/HDPE displayed very decent shape-memory when deformed at temperatures of 140 °C. Shape-fixity ranged from 92.2% for the 70/30 specimen up to 95.5% for the 40/60-blend. Shape recovery values were again highest for the EPDM-rich batch, with up to 97.8%. At 140 °C, the stress necessary for a strain of 50% (255–285 min) was rather similar for all blends having the same mixing ratio. 140 °C was a temperature where all thermoplastic components were molten, and therefore the resistance to deformation is predominantly determined by the cross-linked rubber phase. Consequently, a higher EPDM-content led to higher stress.

Significant differences became evident in the stress data of the different blends while cooling from 140 °C to 20 °C ($t = 285$–297 min) and during the equilibration phase afterwards. For all EPDM/PP-c-PE-samples, as well as for the EPDM/ULDPE (70/30)-sample, the stress needed to maintain a strain of 50% decreased steadily and reached a constant value, i.e., an equilibrated state, afterwards. The decrease was in accordance with the expectation, that cooling and subsequent solidification of the crystalline segments could effectively counteract the retractive elastic forces of the elastomer. In contrast to that, all other blends showed a more or less pronounced increase in stress, that did not even reach a steady state/equilibrium. This was attributed to a combination of i) considerable shrinkage of the samples during cooling/solidification, and ii) significantly higher stiffness of the thermoplastic phase in the ULDPE- and HDPE-blends, respectively, in comparison to the PP-c-PE-blends, and iii) general slow rearrangement of polymer segments or equilibration in the solid state.

Two examples of the macroscopic shape-memory of the investigated blends are shown in Fig. 4D and F. For these examples, rectangular strips with a thickness of 2 mm were cut from vulcanized sheets. A strip of EPDM/ULDPE (40/60) was used to demonstrate dual-shape-memory behavior by applying the cycle illustrated schematically in Fig. 4E.

To show the capability of the investigated materials to perform not only dual-shape-memory, a strip of EPDM/PP-c-PE (40/60) was programmed in two steps. First, a circular shape/deformation was created at $T_{trans,1} = 140$ °C and fixed by cooling to $T_{trans,2} = 60$ °C. At this temperature, the sample was bent into a spiral shape, and subsequently cooled to room temperature for shape fixation. When heated again to 60 °C, recovery of the circular shape occurred. After heating to 140 °C and full recovery, the shape agreed well with the original sample. Thus, the blend can conveniently be programmed into distinct shapes for triple-shape-memory. Within these experiments, shape programming and shape fixation times were set to approximately 10 min. It is worth mentioning that shape recovery, especially when performed in an oil bath for rapid heat transfer and good observability, occurred impressively quickly, within 20–30 s.

3.5. Multi-shape-memory experiments and mechanistic considerations

Reports of triple- as well as quadruple-shape-memory behavior of SMPs based on polymer blends or similar systems have been frequently published [22,24,46,76]. The macroscopic dual- and triple-shape-memory experiments (Fig. 4), as well as the relatively broad thermal transitions (Fig. 2) indicated that 50/50-, and especially 40/60-blends, are promising candidates for thermo-responsive multi--shape-memory materials. Within this work, multi-shape is defined as behavior that allows for the distinct recovery of at least three temporary shapes. Hence, the capability for stepwise recovery triggered by an incremental increase in temperature becomes essential. This was investigated for the 40/60 blends by applying the sequence described in section 2.3.4.2.

In contrast to the experiments discussed above, only one shape-programming sequence ($T_{trans} = 140$ °C, $\varepsilon_{load} = 50\%$, $T_{low} = 20$ °C) was applied to investigate the potential for multi-shape recovery. With the equilibration times mentioned in section 2.3.4.2, the EPDM/ULDPE (40/60)-blend again reached a "stress-equilibrated" state before unloading, and a fixed strain of $\varepsilon_{fix} = 49.3\%$. Shortly before unloading, a still slightly decreasing stress was observed for the EPDM/PP-c-PP (40/60)-blend, which reached a fixed strain of $\varepsilon_{fix} = 50.0\%$. Also in consistency with the results described above, the 40/60-blend with HDPE exhibited increasing stress before unloading. Additionally, the software and control algorithm of the DMTA turned out to be slightly too slow for full compensation of the rapidly increasing stress during and after cooling, which finally resulted in a somewhat reduced fixed stress of $\varepsilon_{fix} = 45.6\%$. Fig. 5 shows the strain-recovery of the 40/60-blends in the thermal range from 55 to 140 °C using incremental heating steps of 2.5 °C, and an equilibration time of 20 min after each step. It is obvious, that the blends with the different thermoplastics exhibited significantly

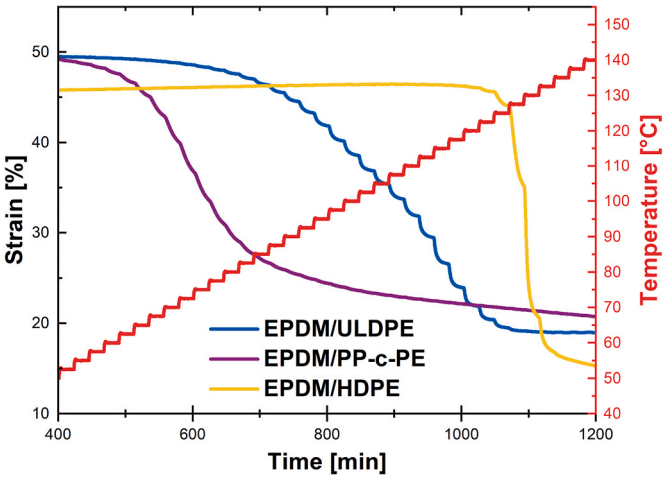

Fig. 5. Direct comparison of thermo-responsive shape recovery (strain vs. temperature) of 40/60-blends of EPDM/PP-c-PE (purple), EPDM/ULDPE (blue), and EPDM/HDPE (yellow); incremental heating after unloading in steps of 2.5 °C; 20 min for equilibration after each step. (For interpretation of the references to colour in this figure legend, the reader is referred to the Web version of this article.)

different recovery. Most of the recovery of EPDM/PP-c-PE (40/60) happened in the thermal range from approx. 60 °C up to 100 °C, while the 40/60-blend with HDPE recovered at higher temperatures, in a rather narrow window, from approx. 115 to 135 °C. In contrast to that, the recovery of EPDM/ULDPE covered a comparably broad thermal range from ca. 60–130 °C. This impressively wide, continuous transition was beneficial with respect to application as temperature indicators (section 3.6).

EPDM/ULDPE (40/60) exhibited hardly visible strain recovery steps at the beginning (approx. 60–65 °C) and subsequently rather small recovery steps per 2.5 °C, which correlates well to the endothermic transitions of ULDPE (Fig. 2B). These strain recovery steps increased and reached a maximum at around 115 °C before decreasing again. It is important to emphasize that i) approximately 20 individual strain recovery steps could be clearly identified, and that ii) all these partial strain recoveries came close to an equilibrated state/strain. Even more steps would be possible by reducing the temperature increment. In contrast to that, the recovery steps of EPDM/PP-c-PP (40/60) did not quite reach an equilibrated strain within the selected equilibration time of 20 min. The material reacted significantly slower. Consequently, the thermal increments were not so clearly resolved in the strain recovery curve. The recovery curve of the 40/60-blend with HDPE showed only a few steps, additionally, equilibration behavior was even slower. Resultantly, from the materials investigated within this work, EPDM/ULDPE (40/60) was the most promising for thermo-responsive multi-shape-memory.

Semantically, due to the non-existence of dedicated multi-shape-programming steps in this particular measurement cycle, the effects discussed above could also be referred to as “thermo-responsive shape recovery” or “temperature-memory”. Nevertheless, the results clearly prove that the material can evidently memorize a multitude of length- or shape-configurations using temperatures over a rather broad range.

A schematic illustration of the expected mechanism and the origin of the recovery of EPDM/ULDPE (40/60) over a broad thermal window is depicted in Fig. 6A. In general, the shape-memory effect in immiscible blends arises from the synergistic interaction of two distinct phases, namely the cross-linked elastomer and the crystalline switching segments [17,77,78]. The initial sample geometry after programming and cooling to room temperature (fixed shape @T_{low}) is determined by the equilibrium of the contractive elastic forces, provided by the cross-linked and strained elastomeric network (EPDM), and the opposing resistance provided by the crystallized thermoplastic domains (ULDPE). While exposing EPDM/ULDPE (40/60) to an incremented increase in temperature, crystalline domains of ULDPE will melt, but only partially, yielding a somewhat reduced resistance/overall internal stress provided by the thermoplastic. As a result, the entropic force provided by the EPDM phase leads to an adequate contraction step of the specimen (intermediate shape). This phenomenon will progress further. Finally, all crystalline regions are melted and the specimen contracts to a completely equilibrated state (recovered shape @T_{high}). At this stage, the internal stress from the thermoplastic domains, as well as the contractive elastic forces are zero. Of course, the contributions of the crystalline segments of EPDM have to be considered too. With regards to the thermal characteristics, the proposed controllable shape-memory mechanism requires a uniquely broad thermal transition, as illustrated by the DSC thermogram in Fig. 6B. The initial endothermic melting transition between ca. 20 and 45 °C was attributed to the crystalline segments of the EPDM phase, as evidenced by the shown thermal data (see Fig. 2B). At temperatures as low as 45–60 °C, ULDPE starts to melt, resulting in a continuous and extraordinarily broad melting peak up to approximately 120 °C.

During the experiment discussed above (Fig. 5), EPDM/ULDPE (40/60) was loaded in a single step (ε_{load} = 50%) at T_{trans} = 140 °C and subsequently cooled directly to T_{min} = 20 °C, which resulted in a fixed strain of ε_{fix} = 49.3%. To investigate the capability of the material to fix additional strains applied at lower temperatures, and to get more insight into the behavior of the blend, the stress-controlled procedure described in section 2.3.4.3 was used. During this sequence, the sample was first heated to T_{trans} = 140 °C and a stress of only 0.04 N mm^{-2} was applied. For EPDM/ULDPE (40/60) this resulted in a strain of 18.9% (Fig. 7A). Subsequently, the temperature was reduced in steps of 20 °C down to a temperature of 60 °C, and the applied stress was increased stepwise to finally 0.7 N mm^{-2}, before strain fixation was completed by cooling to T_{min} = 20 °C. These temperatures (between 60 and 140 °C) were selected in consideration of the rather intriguing wide temperature range that was provided, particularly with the EPDM/ULDPE-blend. In this manner, the thermomechanical and shape-memory behavior could be studied by exploiting the entire temperature transition range. Making sure to yield a reasonable increase in strain in each step, data from previous measurements were used as a reference point for the selection of the stress applied at the different temperatures. After appropriate equilibration, the recovery was investigated by heating to 140 °C, again in steps of 20 °C. Note that until this point, this was a rather normal multi-shape-memory cycle. But, within the procedure applied here, an additional unloading and isothermal time for equilibration were implemented after each cooling step, with the aim of extracting more information about the behavior of the sample. Fig. 7A shows how the strain of the EPDM/ULDPE (40/60)-sample increased in dependence on the applied stress and temperature. Note that the data clearly indicate a significant increase in the strain during cooling, e.g., from 80.5% to 88.0% while the sample was cooled from 60 to 20 °C under a constant stress of 0.7 N mm^{-2}. The behavior was assigned to crystallization-

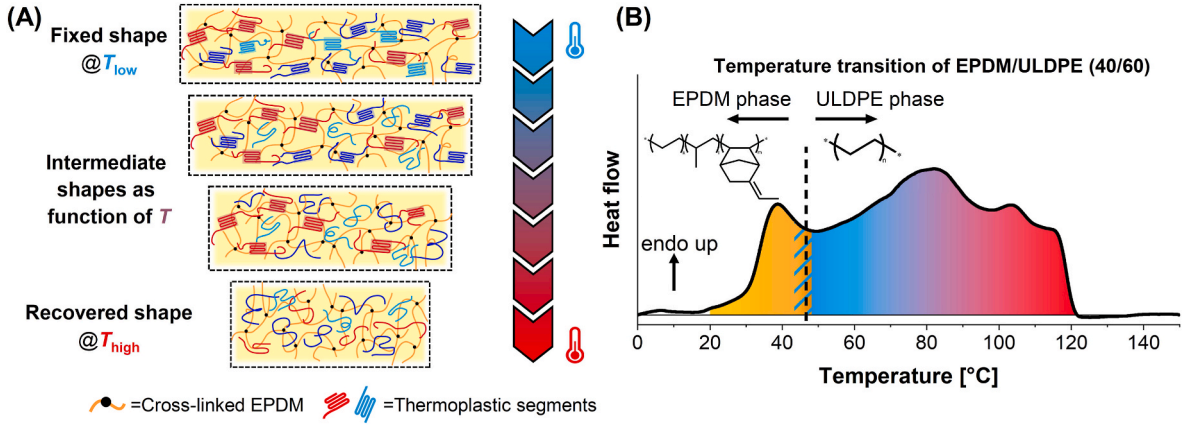

Fig. 6. Expected mechanism for the temperature triggered shape recovery over a broad thermal range observed for EPDM/ULDPE (40/60) programmed with a fixed strain **(A)**; Illustrative DSC-thermogram of EPDM/ULDPE (40/60), indicating the thermal transition ranges applicable for multi-shape recovery **(B)**.

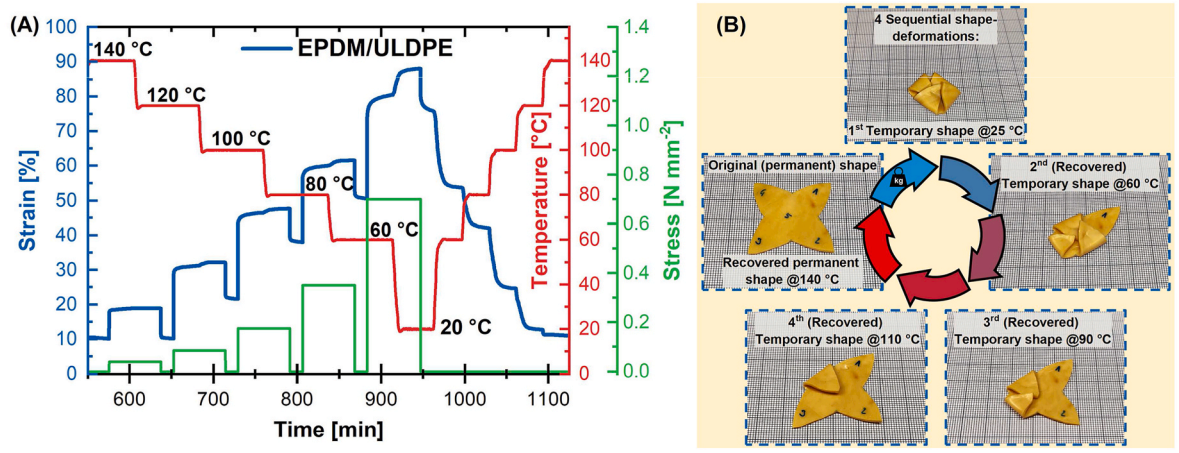

Fig. 7. DMTA data of a stress-controlled multi-shape-memory-experiment (2nd cycle) of EPDM/ULDPE (40/60) **(A)**. Qualitative example for stepwise shape recovery of the same material using a flower-shaped sample **(B)**.

induced elongation (CIE) due to anisotropic chain orientation under strain. Furthermore, the additional unloading steps during the programming sequence of the sample clearly showed that practically no strain was fixed when the sample was cooled to just 120 °C. At this temperature, the ULDPE phase was obviously not stiff enough to fix the applied deformation. As evidenced by the strain-curve progression, the recovered strain at each individual temperature, observed during the stepwise recovery, came very close to the fixed strain values (in the unloaded state) at each individual temperature during programming of the EPDM/ULDPE (40/60)-sample. I.e., directly comparing the fixed strain at the end of the unloading step with the strain at the end of the isothermal recovery step at the corresponding temperatures. For example, an already fixed strain of 38.1% was observed when unloading the sample at 80 °C during the cooling/programming sequence, while the strain recovered after heating to 80 °C was 42.1%. 50.6% vs. 53.7% were the corresponding values at 60 °C. These results clearly show, how well EPDM/ULDPE (40/60) can fix additional strains or shapes applied at various temperatures below 120 °C, and that it is indeed a potent multi-shape-memory material. Obviously, the results presented here benefit from the fact, that the temperatures applied during the whole sequence fit well with the fundamental thermal recovery characteristics of EPDM/ULDPE (40/60) (as shown and discussed in Fig. 5). It should be mentioned that the analogous measurement that was performed without the unloading steps during cooling/programming (the recovery sequence of which is shown in Fig. 8) revealed highly analogous behavior and only minor differences with respect to the stepwise recovery behavior, of only a few percent.

From a practical point of view, the DMTA data imply that four temporary shapes could be clearly resolved, while heating to 120 °C will already give more or less the final recovered shape. For demonstration, Fig. 7B shows images of a corresponding experiment using flower-shaped EPDM/ULDPE (40/60) with four patels. The intermediate shapes of the flower were programmed subsequently by heating the specimen to the deformation temperatures (T_{trans} = 140, 110, 90 and 60 °C; 10 min isothermal) and fixing the individual patels at room temperature (15 min). Slightly different temperature stages in comparison with DMTA measurements were used, as only four instead of five shapes were programmed. These were again derived from the blend's thermal properties (see Fig. 2B). The first picture (top) shows the stable closed flower at ambient conditions. The petals were then opened separately by applying increasing temperature isotherms (10 min) at 60, 90, 110 °C and finally 140 °C, as depicted in the following four pictures (clockwise), to give the fully opened flower again. Note that significantly more temporary shapes would be possible, i.e., by the application of sequences with smaller temperature/deformation steps.

The results indicate that the temperature-stress-pairs applied for

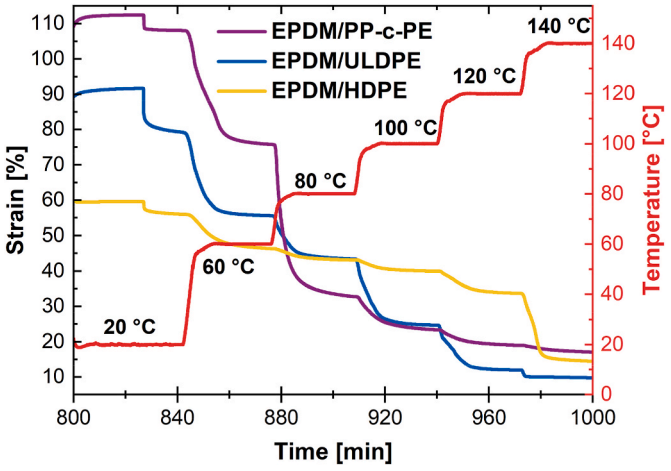

Fig. 8. Direct comparison of the thermo-responsive multi-shape recovery (2nd cycle) of 40/60-blends of EPDM/PP-c-PE (purple), EPDM/ULDPE (blue), and EPDM/HDPE (yellow) after programming of five deformations; samples unloaded at t = 826 min. (For interpretation of the references to colour in this figure legend, the reader is referred to the Web version of this article.)

optimal multi-shape-memory programming of a specific blend must be selected thoughtfully with respect to the stiffness and fundamental thermal recovery behavior of the material (Fig. 5). Consequently, the procedure applied to EPDM/ULDPE (40/60) was anticipated not to be most advantageous for the 40/60-blends containing PP-c-PE and HDPE, respectively. To demonstrate that, all 40/60-blends were investigated with the DMTA-procedure discussed above. The shape-programming temperatures were consciously not changed, but appropriately adjusted stresses had to be applied for EPDM/PP-c-PE (40/60) and EPDM/HDPE (40/60), since the blends had significantly different stiffness. Furthermore, the unloading steps during cooling and programming were skipped. A magnified view of the recovery behavior of the different blends is reproduced in Fig. 8. As already mentioned above, skipping the intermediate unloading/equilibration had only minor effects on the recovery behavior of EPDM/ULDPE (40/60). The material showed a distinct multi-step shape recovery. ULDPE not only possesses a higher degree of crystallinity than PP-c-PE, but it also additionally has a diverse enough crystallite population with seamless solidification temperatures over a remarkably broad range, enabling the fixation and recovery of several temporary deformations. In contrast to that, EPDM/PP-c-PE (40/60) recovered rapidly in about two to three steps. Most of the recovery had already occurred at temperatures as low as 60 and 80 °C. This was

attributed to and is in accordance with the thermal properties of the material, which showed the major melting peak in that temperature region. Subsequent recovered deformation steps were clearly less regular. Note that this fit well with what could be predicted from Fig. 5. Thus, better utilization of the shape-memory potential of EPDM/PP-c-PE (40/60) could only be achieved by programming more stress/temperature pairs below 80 °C. Nonetheless, a recovery of four distinguishable temporary steps for EPDM/ULDPE and three temporary steps for EPDM/PP-c-PE could be demonstrated, effectively concluding their quintuple- and quadruple-shape-memory behavior, respectively. Regarding EPDM/HDPE (40/60), shape programming should mainly be done in smaller increments at higher temperatures, since the blend showed major shape recovery at the last two temperatures of 120 and 140 °C in accordance with its rather sharp melting transition between 110 and 135 °C and for that reason would be less attractive for applications requiring a broad thermal range. However, an additional and significant shape recovery step was also observed at 60 °C, which was induced by the crystalline phase of the EPDM. The applied semi-crystalline EPDM type exhibited a degree of crystallinity of up to $X_c = 8\%$ (evaluation shown in Fig. S9).

3.6. Application of EPDM/ULDPE (40/60) as temperature indicator

The gradual and reproducible temperature-dependent shape recovery of the EPDM/ULDPE-blend opens the possibility for application as temperature-indicating material in the range from 80 to 135 °C. Consequently, corresponding experiments on macroscopic samples were performed. Sample strips of 100 mm × 10 mm were cut and subjected to an initial shape-memory cycle (initial heating to 140 °C, applying 50% strain, fixation at room temperature and subsequent recovery), in order to obtain a substantially stress-free material and to erase the thermal history. After this conditioning step, the material was heated again to 140 °C. The marked section (as shown in Fig. 9) was strained to 50% and the deformation was fixed at room temperature. The obtained test strips could be stored at ambient temperatures for weeks without undergoing a significant change in length. Starting with an initial marked length of approximately 120 mm, the strips were heated first to 60 °C, and then sequentially in steps of 10 °C up to 140 °C. The exposure time at each temperature was 15 min. A complete temperature-indication experiment is illustrated in Fig. 9. The indicated length (or remaining fixed strain) of the sample, especially between about 80 and 120 °C, could easily be quantified.

It depicts the results of an experiment where the temperature was increased stepwise. In a control experiment, samples were heated to one single target temperature at a time, and the length was determined. A comparison of the recovered strains using "stepwise" temperature recovery versus a single targeted step is summarized in Table 3. It must be emphasized that the deformation process within these preliminary temperature-sensing experiments was done manually and individually for each sample strip, which potentially introduces an additional source of error. Machine-controlled heating and deformation steps would probably reduce error margins significantly.

4. Conclusion

In conclusion, combining EPDM and polyolefin thermoplastics (PP-c-PE, ULDPE or HDPE) in binary blends, allowed for the fabrication of effective dual- and triple-shape-memory materials from commodity raw components. Structurally, vulcanized EPDM forms a cross-linked rubber network, acting as the fixed phase, while the thermoplastic components provide the crystalline switching segments. Thermal characterization revealed the presence of immiscible binary elastomer-thermoplastic-blends. EPDM/ULDPE showed a phase separation with a seemingly co-continuous morphology, as furtherly evidenced by AFM measurements, facilitating the proposed mechanism. The found phase-separated morphologies were in accordance with previous investigations on similar measurements on EPDM/HDPE- and EPDM/PP-c-PE-blends [75]. Fundamental shape-memory-behavior of blends with the different thermoplastics, as examined with dynamic-mechanical thermal analysis, could be correlated with the inherent material properties. In consideration of the systematic variation in blend ratios, it could be concluded that the thermoplastic content had a significant impact on the mechanical properties, i.e., a higher content of thermoplastic led to improved performance. Since the produced blends were immiscible, no influence of the blending ratio on the thermal transitions could be affirmed. The shape-memory properties in dual-shape-cycles were generally improved with increasing thermoplastic content. This held especially true for shape-fixity, as it was promoted by the thermoplastic

Table 3
Recovered strain of test strips after stepwise temperature increase (steps at 10 °C, multiple determination, 5x) in comparison to direct heating to single target temperatures.

Temperature [°C]	Recovered Strain (stepwise increase to final *T*)	Recovered Strain (direct heating to target *T*)
70	46 ± 2%	46.2%
80	44 ± 2%	44.4%
90	38 ± 2%	36.4%
100	27 ± 2%	29.2%
110	11 ± 3%	14.1%
120	0 ± 3%	1.0%
130	−3 ± 4%	−0.5%

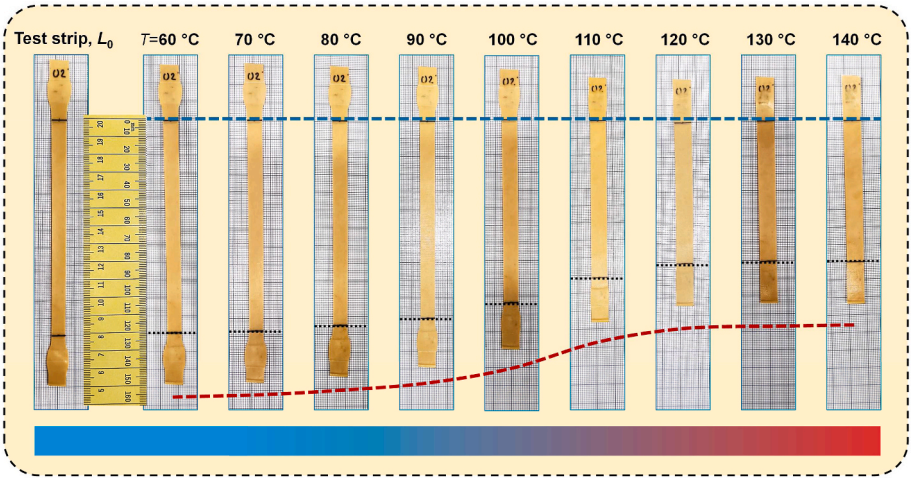

Fig. 9. Temperature-indication experiment with an EPDM/ULDPE (40/60) test strip with stepwise temperature increase (increments 10 °C).

switching segments, while sufficient entropy elastic energy for shape recovery was still provided by the cross-linked EPDM. The most promising material combination, EPDM/ULDPE (40/60), with a unique broad thermal transition ranging from 40 °C to 125 °C, enabled the realization of multi-shape-memory. Quintuple-shape-memory and shape-recovery with an even higher multitude of temporary shapes was successfully demonstrated on macroscopic samples and using dynamic-mechanical thermal analysis, respectively. DMTA-experiments on a shape-memory-blend based on the same material showed a continuous recovery behavior starting at approximately 60 °C and continuing to 125 °C. The underlying mechanism is based on the interaction between a cross-linked rubber phase and crystalline switching segments melting at different temperatures, making these materials interesting as an indicator of the maximum exposure temperature.

In a real-world practical application, the measured length of these conditioned, one-way, reusable test strips was used to infer and display the maximum exposure temperature in their immediate vicinity. Possible applications include controlling cooling chains, monitoring high temperatures during transportation and shipment, and implementing the material for overheating protection in buildings.

CRediT (contributor roles taxonomy) author statement

Reinhold Pommer: Conceptualization, Methodology, Validation, Formal analysis, Investigation, Resources, Data Curation, Writing - Original Draft, Visualization. Robert Saf: Conceptualization, Methodology, Validation, Formal analysis, Investigation, Resources, Data Curation, Writing - Original Draft, Writing - Review & Editing. Ralf Supplit: Resources, Writing - Review & Editing. Armin Holzner: Resources, Writing - Review & Editing, Project administration. Harald Plank: Formal analysis, Investigation, Writing - Review & Editing. Gregor Trimmel: Conceptualization, Validation, Resources, Data Curation, Writing - Original Draft, Writing - Review & Editing, Supervision, Project administration, Funding acquisition.

Declaration of competing interest

The authors declare that they have no known competing financial interests or personal relationships that could have appeared to influence the work reported in this paper.

Data availability

The authors do not have permission to share data.

Acknowledgements

The research work was performed within the COMET-project "*Tuning the Shape-Memory-Effect in Elastomer-Thermoplast Blends*" (project-no.: VII-1.04) at the Polymer Competence Center Leoben GmbH (PCCL, Austria) within the framework of the COMET-program of the Federal Ministry for Climate Action, Environment, Energy, Mobility, Innovation and Technology and the Federal Ministry for Digital and Economic Affairs with contributions by Graz University of Technology (Institute for Chemistry and Technology of Materials) and Semperit Technische Produkte GmbH. The PCCL is funded by the Austrian Government and the State Governments of Styria, Lower Austria and Upper Austria. The authors acknowledge the financial support by the Austrian Federal Ministry for Digital and Economic Affairs and the National Foundation for Research, Technology, and Development (Christian Doppler Laboratory DEFINE, Austria)

Appendix A. Supplementary data

Supplementary data to this article can be found online at https://doi.org/10.1016/j.polymer.2023.126302.

References

[1] J. Hu, Introduction to shape memory polymers, in: Advances in Shape Memory Polymers, Woodhead Publishing, 2013, pp. 1–22.
[2] M. Behl, A. Lendlein, Shape-memory polymers, mater, Today Off. 10 (2007) 20–28, https://doi.org/10.1016/S1369-7021(07)70047-0.
[3] P.T. Mather, X. Luo, I.A. Rousseau, Shape memory polymer research, Annu. Rev. Mater. Res. 39 (2009) 445–471, https://doi.org/10.1146/annurev-matsci-082908-145419.
[4] S. Jose, J.J. George, S. Siengchin, J. Parameswaranpillai, Introduction to shape-memory polymers, polymer blends and composites: state of the art, opportunities, new challenges and future outlook, in: J. Parameswaranpillai (Ed.), Shape Memory Polymers, Blends and Composites, Springer, Singapore, 2020, pp. 1–19.
[5] K. Strzelec, N. Sienkiewicz, T. Szmechtyk, Classification of shape-memory polymers, polymer blends, and composites, in: J. Parameswaranpillai (Ed.), Shape Memory Polymers, Blends and Composites, Springer, Singapore, 2020, pp. 21–52.
[6] T. Xie, Recent advances in polymer shape memory, Polymer 52 (2011) 4985–5000, https://doi.org/10.1016/j.polymer.2011.08.003.
[7] L. Sun, W.M. Huang, Z. Ding, Y. Zhao, C.C. Wang, H. Purnawali, C. Tang, Stimulus-responsive shape memory materials: a review, Mater. Des. 33 (2012) 577–640, https://doi.org/10.1016/j.matdes.2011.04.065.
[8] J. Jia, N. Gao, R. Li, S. Liao, S. Lyu, Y. Wang, An "OFF-to-ON" shape memory polymer conductor for early fire disaster alarming, Chem. Eng. J. 431 (2022), 133285, https://doi.org/10.1016/j.cej.2021.133285.
[9] F. Pilate, A. Toncheva, P. Dubois, J.-M. Raquez, Shape-memory polymers for multiple applications in the materials world, Eur. Polym. J. 80 (2016) 268–294, https://doi.org/10.1016/j.eurpolymj.2016.05.004.
[10] L. Sun, T.X. Wang, H.M. Chen, A.V. Salvekar, B.S. Naveen, Q. Xu, Y. Weng, X. Guo, Y. Chen, W.M. Huang, A brief review of the shape memory phenomena in polymers and their typical sensor applications, Polymers 11 (2019) 1049, https://doi.org/10.3390/polym11061049.
[11] J. Li, Q. Duan, E. Zhang, J. Wang, Applications of shape memory polymers in kinetic buildings, Adv. Mater. Sci. Eng. (2018) 1–13, https://doi.org/10.1155/2018/7453698, 2018.
[12] W.M. Sokolowski, S.C. Tan, Advanced self-deployable structures for space applications, J. Spacecraft Rockets 44 (2007) 750–754, https://doi.org/10.2514/1.22854.
[13] L. Santo, F. Quadrini, D. Bellisario, L. Iorio, Applications of shape-memory polymers, and their blends and composites, in: J. Parameswaranpillai (Ed.), Shape Memory Polymers, Blends and Composites, Springer, Singapore, 2020, pp. 311–329.
[14] J. Hu, Y. Zhu, H. Huang, J. Lu, Recent advances in shape–memory polymers: structure, mechanism, functionality, modeling and applications, Prog. Polym. Sci. 37 (2012) 1720–1763, https://doi.org/10.1016/j.progpolymsci.2012.06.001.
[15] Y. Chen, C. Chen, H.U. Rehman, X. Zheng, H. Li, H. Liu, M.S. Hedenqvist, Shape-memory polymeric artificial muscles: mechanisms, applications and challenges, Molecules 25 (2020) 4246, https://doi.org/10.3390/molecules25184246.
[16] Y. Xia, Y. He, F. Zhang, Y. Liu, J. Leng, A review of shape memory polymers and composites: mechanisms, materials, and applications, Adv. Mater. 33 (2021), 2000713, https://doi.org/10.1002/adma.202000713.
[17] Q. Meng, J. Hu, A review of shape memory polymer composites and blends, Compos. Part A Appl. Sci. Manuf. 40 (2009) 1661–1672, https://doi.org/10.1016/j.compositesa.2009.08.011.
[18] H. Meng, G. Li, A review of stimuli-responsive shape memory polymer composites, Polymer 54 (2013) 2199–2221, https://doi.org/10.1016/j.polymer.2013.02.023.
[19] S. Salaeh, A. Das, S. Wießner, Design and fabrication of thermoplastic elastomer with ionic network: a strategy for good performance and shape memory capability, Polymer 223 (2021), 123699, https://doi.org/10.1016/j.polymer.2021.123699.
[20] A. Basit, G. L'Hostis, B. Durand, Multi-shape memory effect in shape memory polymer composites, Mater. Lett. 74 (2012) 220–222, https://doi.org/10.1016/j.matlet.2012.01.113.
[21] K. Wang, Y.-G. Jia, C. Zhao, X.X. Zhu, Multiple and two-way reversible shape memory polymers: design strategies and applications, Prog. Mater. Sci. 105 (2019), 100572, https://doi.org/10.1016/j.pmatsci.2019.100572.
[22] C. Samuel, S. Barrau, J.-M. Lefebvre, J.-M. Raquez, P. Dubois, Designing multiple-shape memory polymers with miscible polymer blends: evidence and origins of a triple-shape memory effect for miscible PLLA/PMMA blends, Macromolecules 47 (2014) 6791–6803, https://doi.org/10.1021/ma500846x.
[23] Q. Zhao, M. Behl, A. Lendlein, Shape-memory polymers with multiple transitions: complex actively moving polymers, Soft Matter 9 (2013) 1744–1755, https://doi.org/10.1039/C2SM27077C.
[24] T. Xie, Tunable polymer multi-shape memory effect, Nature 464 (2010) 267–270, https://doi.org/10.1038/nature08863.
[25] M. Kashif, Y.-W. Chang, Triple-shape memory effects of modified semicrystalline ethylene–propylene–diene rubber/poly(ε-caprolactone) blends, Eur. Polym. J. 70 (2015) 306–316, https://doi.org/10.1016/j.eurpolymj.2015.07.026.
[26] L. Yang, J. Lou, J. Yuan, J. Deng, A review of shape memory polymers based on the intrinsic structures of their responsive switches, RSC Adv. 11 (2021) 28838–28850, https://doi.org/10.1039/d1ra04434f.
[27] Y. Zhou, W.M. Huang, Shape memory effect in polymeric materials: mechanisms and optimization, Procedia IUTAM 12 (2015) 83–92, https://doi.org/10.1016/j.piutam.2014.12.010.
[28] A. Lendlein, O.E.C. Gould, Reprogrammable recovery and actuation behaviour of shape-memory polymers, Nat. Rev. Mater. 4 (2019) 116–133, https://doi.org/10.1038/s41578-018-0078-8.

[29] C. Liu, H. Qin, P.T. Mather, Review of progress in shape-memory polymers, J. Mater. Chem. 17 (2007) 1543, https://doi.org/10.1039/B615954K.
[30] X. Xin, L. Liu, Y. Liu, J. Leng, Mechanical models, structures, and applications of shape-memory polymers and their composites, Acta Mech. Solida Sin. 32 (2019) 535–565, https://doi.org/10.1007/s10338-019-00103-9.
[31] Y. Tian, Q. Wang, Y. Hu, H. Sun, Z. Cui, L. Kou, J. Cheng, J. Zhang, Preparation and shape memory properties of rigid-flexible integrated epoxy resins via tunable micro-phase separation structures, Polymer 178 (2019), 121592, https://doi.org/10.1016/j.polymer.2019.121592.
[32] H. Zhuo, X. Huang, W. Dai, H. Chen, S. Chen, Preparation of self-healing shape memory polymer based on crystalline side chain, Mater. Lett. 308 (2022), 131300, https://doi.org/10.1016/j.matlet.2021.131300.
[33] M. Pantoja, P.-Z. Jian, M. Cakmak, K.A. Cavicchi, Shape memory properties of polystyrene- block -poly(ethylene- co -butylene)- block -polystyrene (SEBS) ABA triblock copolymer thermoplastic elastomers, ACS Appl. Polym. Mater. 1 (2019) 414–424, https://doi.org/10.1021/acsapm.8b00139.
[34] X. Qi, Y. Wang, Novel techniques for the preparation of shape-memory polymers, polymer blends and composites at micro and nanoscales, in: J. Parameswaranpillai (Ed.), Shape Memory Polymers, Blends and Composites, Springer, Singapore, 2020, pp. 53–83.
[35] R. Zende, V. Ghase, V. Jamdar, A review on shape memory polymers, Polym. Plast. Technol. Mater. 62 (2023) 467–485, https://doi.org/10.1080/25740881.2022.2121216.
[36] Y. Gao, W. Liu, S. Zhu, Thermoplastic polyolefin elastomer blends for multiple and reversible shape memory polymers, Ind. Eng. Chem. Res. 58 (2019) 19495–19502, https://doi.org/10.1021/acs.iecr.9b03979.
[37] E. Tekay, Thermo-responsive shape memory behavior of poly(styrene-b-isoprene-b-styrene)/ethylene-1-octene copolymer thermoplastic elastomer blends, Polym. Adv. Technol. 32 (2021) 428–438, https://doi.org/10.1002/pat.5139.
[38] Z. Zhang, J. Du, W. Shan, T. Ren, Z. Lu, A facile approach toward thermoplastic triple-shape memory polymers, Macromol. Mater. Eng. 306 (2021), 2000508, https://doi.org/10.1002/mame.202000508.
[39] B. Zeng, M. Cao, J. Shen, K. Yang, Y. Zheng, S. Guo, Tuning the dual- and triple-shape-memory effect of thermoplastic polyurethane/polylactic acid/poly (propylene carbonate) ternary blends via morphology control, Polymer 242 (2022), 124546, https://doi.org/10.1016/j.polymer.2022.124546.
[40] Y. Chen, K. Chen, Y. Wang, C. Xu, Biobased heat-triggered shape-memory polymers based on polylactide/epoxidized natural rubber blend system fabricated via peroxide-induced dynamic vulcanization: Co-continuous phase structure, shape memory behavior, and interfacial compatibilization, Ind. Eng. Chem. Res. 54 (2015) 8723–8731, https://doi.org/10.1021/acs.iecr.5b02195.
[41] C. Xu, R. Cui, Y. Chen, J. Ding, Shape memory effect of dynamically vulcanized ethylene-propylene-diene rubber/polypropylene blends realized by in-situ compatibilization of sodium methacrylate, Compos. B Eng. 179 (2019), 107532, https://doi.org/10.1016/j.compositesb.2019.107532.
[42] T. Chatterjee, P. Dey, G.B. Nando, K. Naskar, Thermo-responsive shape memory polymer blends based on alpha olefin and ethylene propylene diene rubber, Polymer 78 (2015) 180–192, https://doi.org/10.1016/j.polymer.2015.10.007.
[43] A. Reghunadhan, K.P. Jibin, A.V. Kaliyathan, P. Velayudhan, M. Strankowski, S. Thomas, Shape memory materials from rubbers, Materials 14 (2021) 7216, https://doi.org/10.3390/ma14237216.
[44] I.S. Kolesov, H.-J. Radusch, Multiple shape-memory behavior and thermal-mechanical properties of peroxide cross-linked blends of linear and short-chain branched polyethylenes, Express Polym. Lett. 2 (2008) 461–473, https://doi.org/10.3144/expresspolymlett.2008.56.
[45] M. Tian, W. Gao, J. Hu, X. Xu, N. Ning, B. Yu, L. Zhang, Multidirectional triple-shape-memory polymer by tunable cross-linking and crystallization, ACS Appl. Mater. Interfaces 12 (2020) 6426–6435, https://doi.org/10.1021/acsami.9b19448.
[46] S. Chen, Q. Zhang, J. Feng, 3D printing of tunable shape memory polymer blends, J. Mater. Chem. C 5 (2017) 8361–8365, https://doi.org/10.1039/C7TC02534C.
[47] J. Wang, Z. Tu, H. Zhang, M.-M. Wang, W. Liu, J.-P. Qu, Actuation mechanisms of a semicrystalline elastomer-based polymer artificial muscle with high actuation strain, Macromolecules 55 (2022) 3986–3999, https://doi.org/10.1021/acs.macromol.2c00549.
[48] J. Wang, H. Zhang, J. Lei, M. Wu, W. Liu, J.-P. Qu, Stress-free two-way shape-memory mechanism of a semicrystalline network with a broad melting transition, Macromolecules 55 (2022) 10113–10123, https://doi.org/10.1021/acs.macromol.2c01971.
[49] L. Min, M. Zhu, H. Lu, Y. Li, L. Fan, M. Zhang, M. Rong, Stepless shape morphing polymer, SmartMat 1134 (2022), https://doi.org/10.1002/smm2.1134 smm2.
[50] Y. Li, L. Min, J.H. Xin, L.H. Wang, Q.H. Wu, L.F. Fan, F. Gan, H. Yu, High-performance fibrous artificial muscle based on reversible shape memory UHMWPE, J. Mater. Res. 20 (2022) 7–17, https://doi.org/10.1016/j.jmrt.2022.07.045.
[51] Z. Bartczak, A. Galeski, Mechanical properties of polymer blends, in: L.A. Utracki, C.A. Wilkie (Eds.), Polymer Blends Handbook, Springer Netherlands, Dordrecht, 2014, pp. 1203–1297.
[52] V. Tanrattanakul, W. Udomkichdecha, Development of novel elastomeric blends containing natural rubber and ultra-low-density polyethylene, J. Appl. Polym. Sci. 82 (2001) 650–660, https://doi.org/10.1002/app.1893.
[53] H. Yao, J. Niu, J. Zhang, N. Ning, X. Yang, M. Tian, X. Sun, L. Zhang, S. Yan, Morphologies and mechanical properties of cis-1,4-butadiene rubber/polyethylene blends, Chin. J. Polym. Sci. 34 (2016) 820–829, https://doi.org/10.1007/s10118-016-1794-4.
[54] W. Hofmann, Rubber Technology Handbook, first ed., Hanser, Munich, 1989.
[55] L.M. Robeson, Polymer Blends: A Comprehensive Review, Hanser, Munich, 2007.
[56] I. Fortelný, J. Kovář, A. Sikora, D. Hlavatá, Z. Kruliš, Z. Nováková, Z. Pelzbauer, P. Čefelín, The structure of blends of polyethylene and polypropylene with EPDM elastomer, Angew. Makromol. Chem. 132 (1985) 111–122, https://doi.org/10.1002/apmc.1985.051320109.
[57] S.F. Xavier, Properties and performance of polymer blends, in: L.A. Utracki, C. A. Wilkie (Eds.), Polymer Blends Handbook, Springer Netherlands, Dordrecht, 2014, pp. 1031–1201.
[58] R.A. Shanks, I. Kong, General purpose elastomers: structure, Chemistry, physics and performance, in: P.M. Visakh, S. Thomas, A.K. Chandra, A.P. Mathew (Eds.), Advances in Elastomers I, Springer Berlin Heidelberg, Berlin, Heidelberg, 2013, pp. 11–45.
[59] S. Howse, C. Porter, T. Mengistu, I. Petrov, R.J. Pazur, Experimental determination of the quantity and distribution of chemical crosslinks in unaged and aged natural rubber. II: a sulfur donor system, Rubber Chem. Technol. 92 (2019) 513–530, https://doi.org/10.5254/rct.19.81473.
[60] J. Kruželák, R. Sýkora, I. Hudec, Sulphur and peroxide vulcanisation of rubber compounds – overview, Chem. Pap. 70 (2016) 1533–1555, https://doi.org/10.1515/chempap-2016-0093.
[61] P. Ghosh, B. Chattopadhyay, A.K. Sen, Thermoplastic elastomers from blends of polyethylene and ethylene-propylene-diene rubber: influence of vulcanization technique on phase morphology and vulcanizate properties, Polymer 35 (1994) 3958–3965, https://doi.org/10.1016/0032-3861(94)90281-X.
[62] A. Karekar, R. Pommer, B. Prem, C. Czibula, C. Teichert, G. Trimmel, K. Saalwächter, NMR-based cross-link densities in EPDM and EPDM/ULDPE blend materials and correlation with mechanical properties, Macromol. Mater. Eng. (2022), 2100968, https://doi.org/10.1002/mame.202100968.
[63] J. Karger-Kocsis, L. Kiss, Dynamic mechanical properties and morphology of polypropylene block copolymers and polypropylene/elastomer blends, Polym. Eng. Sci. 27 (1987) 254–262, https://doi.org/10.1002/pen.760270404.
[64] J. Kolařík, J. Velek, G.L. Agrawal, I. Fortelný, Dynamic mechanical behavior and structure of ternary blends of polypropylene/EPDM rubber/polyethylene, Polym. Compos. 7 (1986) 472–479, https://doi.org/10.1002/pc.750070612.
[65] J. Kolařík, G.L. Agrawal, Z. Kruliš, J. Kovář, Dynamic mechanical behavior of binary blends polyethylene/EPDM rubber and polypropylene/EPDM rubber, Polym. Compos. 7 (1986) 463–471, https://doi.org/10.1002/pc.750070611.
[66] J. Parameswaranpillai, H. Pulikkalparambil, M.R. Sanjay, S. Siengchin, Polypropylene/high-density polyethylene based blends and nanocomposites with improved toughness, Mater. Res. Express 6 (2019), 075334, https://doi.org/10.1088/2053-1591/ab18cd.
[67] K.P. Tchomakov, B.D. Favis, M.A. Huneault, M.F. Champagne, F. Tofan, Mechanical properties and morphology of ternary PP/EPDM/PE blends, Can. J. Chem. Eng. 83 (2005) 300–309, https://doi.org/10.1002/cjce.5450830216.
[68] B. Pukánszky, F. Tüdős, Miscibility and mechanical properties of polymer blends, Macromol. Symp. 38 (1990) 221–231, https://doi.org/10.1002/masy.19900380118.
[69] H. Veenstra, P.C. Verkooijen, B.J. van Lent, J. van Dam, A.P. de Boer, A.P. H. Nijhof, On the mechanical properties of co-continuous polymer blends: experimental and modelling, Polymer 41 (2000) 1817–1826, https://doi.org/10.1016/S0032-3861(99)00337-7.
[70] C.M. Roland, Immiscible rubber blends, in: P.M. Visakh, S. Thomas, A.K. Chandra, A.P. Mathew (Eds.), Advances in Elastomers I, Springer Berlin Heidelberg, Berlin, Heidelberg, 2013, pp. 167–181.
[71] F.S. Bates, Polymer-polymer phase behavior, Science 251 (1991) 898–905, https://doi.org/10.1126/science.251.4996.898.
[72] C. Cazan, A. Duta, Rubber/thermoplastic blends: micro and Nano structured, in: P. M. Visakh, S. Thomas, A.K. Chandra, A.P. Mathew (Eds.), Advances in Elastomers I, Springer Berlin Heidelberg, Berlin, Heidelberg, 2013, pp. 183–228.
[73] E. Manias, L.A. Utracki, Thermodynamics of polymer blends, in: L.A. Utracki, C. A. Wilkie (Eds.), Polymer Blends Handbook, Springer Netherlands, Dordrecht, 2014, pp. 171–289.
[74] T. Ougizawa, T. Inoue, Morphology of polymer blends, in: L.A. Utracki, C.A. Wilkie (Eds.), Polymer Blends Handbook, Springer Netherlands, Dordrecht, 2014, pp. 875–918.
[75] B. Prem, Investigation of the Phase Morphology and Mechanical Properties of Elastomer-Thermoplastic Blends, Doctoral Thesis, Graz University of Technology, 2020.
[76] M. Amini, S. Wu, Designing a polymer blend nanocomposite with triple shape memory effects, Compos. Commun. 23 (2021), 100564, https://doi.org/10.1016/j.coco.2020.100564.
[77] S.K. Melly, L. Liu, Y. Liu, J. Leng, Active composites based on shape memory polymers: overview, fabrication methods, applications, and future prospects, J. Mater. Sci. 55 (2020) 10975–11051, https://doi.org/10.1007/s10853-020-04761-w.
[78] H. Zhang, H. Wang, W. Zhong, Q. Du, A novel type of shape memory polymer blend and the shape memory mechanism, Polymer 50 (2009) 1596–1601, https://doi.org/10.1016/j.polymer.2009.01.011.